Technical Physics, 2022, Vol. 67, No. 6

03

High-speed low-temperature gas analyzer for pulsed emissions of liquefied natural gas into the atmosphere based on immersion diode optocouplers

© *A.V. Zagnit'ko,*[1] *I.D. Matsukov,*[2] *V.V. Pimenov,*[1] *S.E. Sal'nikov,*[1] *D.Yu. Fedin,*[1] *V.I. Alekseev,*[2]
S.M. Vel'makin[1]

[1] National Research Center „Kurchatov Institute", Moscow, Russia
[2] Priozersky Branch of the National Research Center „Kurchatov Institute", Moscow, Russia
e-mail: zagnitko_av@nrcki.ru

Received December 24, 2021
Revised March 3, 2022
Accepted March 4, 2022

A low-temperature infrared optical gas analyzer based on immersion diode optocouplers with a speed of less than 0.03 s has been developed to detect pulsed emissions into the atmosphere of explosive mixtures of liquefied natural gas and alkanes with air at a temperature of more than 150 K with the transfer of digitized data to a remote server. The design is described and its characteristics are given in the process of analyzing mixtures of air with pure methane, ethane, propane and LNG of various compositions. It is shown that the speed and operating temperature range of the gas analyzer exceed the parameters of foreign and domestic analogues for monitoring man-made LNG emissions into the atmosphere.

Keywords: alkanes, speed, infrared optical gas analyzer, pulse emissions, immersion diode optocouplers, liquefied natural gas.

DOI: 10.21883/0000000000

Introduction

When ensuring industrial safety of production and storage facilities of liquified natural gas (LNG), it is required to evaluate consequences of their man-made pulse emissions as jets and ground spillage with liquid-carbohydrate regasification formation of fire hazardous clouds of air fuel mixtures (AFM) with volume concentration inflammation limits (CIL) within the range from 5 to 15 vol.% [1–3]. It is quite difficult to analyze them as it is required to measure fluctuating values of the concentration C at the temperature of $T \geq 150$ K with transmission of the digital data to the remote server, while the devices for scanning the AFM clouds must have a speed $\tau < 0.1$ s, function at the velocity of gas-drop fluxes up to hundreds meters per second and be resistive to the gas pressure pulses of up to 10^5 Pa [2–14]. Here, τ is determined as the time required to measure the volume concentration of the gas mixture at 90% of its final value after fast change of the value C.

It is known that for the industrial semiconductor gas analyzers based on the metal dioxide films doped with palladium, copper oxide, etc., the value $\tau \leq 2-3$ s due to a relatively small rate of diffusion of the analyzed molecules through the sensitive thin film of the metal dioxide [4–7]. The efforts to improve their speed due to optimization of its thickness and chemical composition, the heating temperature and the stabilization diagram allowed designing prototypes with 0.3 s.

The electrochemical gas analyzers are designed to perform a selective reaction of the analyzed molecules with the electrolyte [4–7]. The generated current is directly proportional to the concentration of the detected gas and the value $\tau = 15-30$ s [4–7].

In the typical infrared optical (IR) gas analyzers, for example, Sensis-500 with a foreign pyroelectric sensor of the „MSH-P-CH4-5BPF Dynament GB" type and carbohydrate molecular absorption of IR radiation with the operating wavelength of $\lambda = 3.3\,\mu$m of an tungsten-filament incandescent lamp, the analyzed gases are taken by their molecular diffusion through a protection aerosol filter of the sensor [8]. As a result, $\tau \approx 20-25$ s at the temperature above 255 K.

The domestic IR gas analyzers based on the „Mipex" sensors using traditional light-emitting diodes and photodiodes with aerosol filters are characterized by the value $\tau \approx 0.5-1$ s at $T > 150$ K due to creating a pre-heated electric furnace flux of convective diffusion of a detected gas mixture through the sensor by means of an aspirator [9–11].

In the said IR analogues, the light-emitting diodes with a wide radiation diagram and the photodiodes are rigidly joined to a body of the gas cuvette [7–11]. It is not critical as the most of IR radiation is collected at a photodetector. However, with the narrow directivity diagrams for light-emitting diode's radiation and its photodiode reception, which are typical for the immersion diode optocouplers, their position is fixed by means of a flexible mechanical connection with the gas cuvette body by adjusting elements, as the diagram of source radiation propagation is not necessarily coincident with the sensitivity maximum of the photodetector radiation reception diagram [12–14].

At the same time, the IR gas analyzers based on the immersion diode optocouplers are designed to measure the concentration of the carbohydrates with the speed up to 0.1 s [12–14]. However, the latter can not detect vaporization of methane emissions and the wide fraction of light hydrocarbons (LHWF: ethane, propane, butane and other light alkanes) of LNG into the atmosphere with a typical time of fluctuations of their volume concentration below 0.1 s at $T > 150$ K. It is due to the fact that the immersion diode optocouplers are not designed to operate at such a low temperature.

The purpose of the present study was to develop the low-temperature IR gas analyzer based on the immersion diode optocouplers for express-monitoring of man-made and natural pulse emissions of alkanes and LNG as flooded jets or ground spills with formation of fluctuating explosive and fire hazardous AFM concentrations during the liquid hydrocarbon regasification with the speed $\tau < 0.03$ s at the temperature above 150 K [1]. It has investigated the dependence of vaporization of fine particles of liquid alkanes on their diameter and the atmosphere temperature.

1. Experimental part

Figure 1 shows the principle diagram and the image of the patented high-speed low-temperature IR gas analyzer of pulse emissions of alkanes and LNG into the atmosphere based on the immersion diode optocouplers [15].

The device includes the flow activator Q of the analyzed carbon-air mixture 8 through the measurement gas cuvette *1*, whose reflecting surfaces form an optical diagram for generation of the IR radiation beam, its source as the immersion light-emitting diode *9* and its photodetector as the immersion photodiode *10* [12–14], which are connected by the flexible mechanical connection to the body *2* of the gas cuvette with the adjusting elements *11* and *12*, the external electronic units *14* and *15* for power supply, control, stabilization of the temperature and transmission of the digitalized signals to the remote server for analysis thereof. The body of the gas cuvette *1* is made with the external heat-insulation coating *3* and mechanically mated to the cylindrical channel of the electric oven *4* for heating and inputting the analyzed gas into the gas cuvette *1*. The internals of the cylindrical channel of the electric oven have the aerosol metal filter *5* and the thermocouple *7* installed in series in order to control the temperature of the analyzed AFM. Externally, it also includes the thermocouple *6* for analysis of its outside temperature. The electronic unit *15* includes a board for control of the chromel-alumel thermocouples *6* and *7*, the flow activator *8* and the cylindrical electric oven *4*. The fibrous aerosol metal filter *5* of the H11 class is made of copper with the particle trapping efficiency above 99.9%. The heat insulation *3* is made of synthetic expanded rubber to reduce heat exchange between the external atmosphere and the internal volume of the gas cuvette *1*. In special cases, the screen-vacuum heat insulation of the pressure of at most 10^{-6} Pa is used.

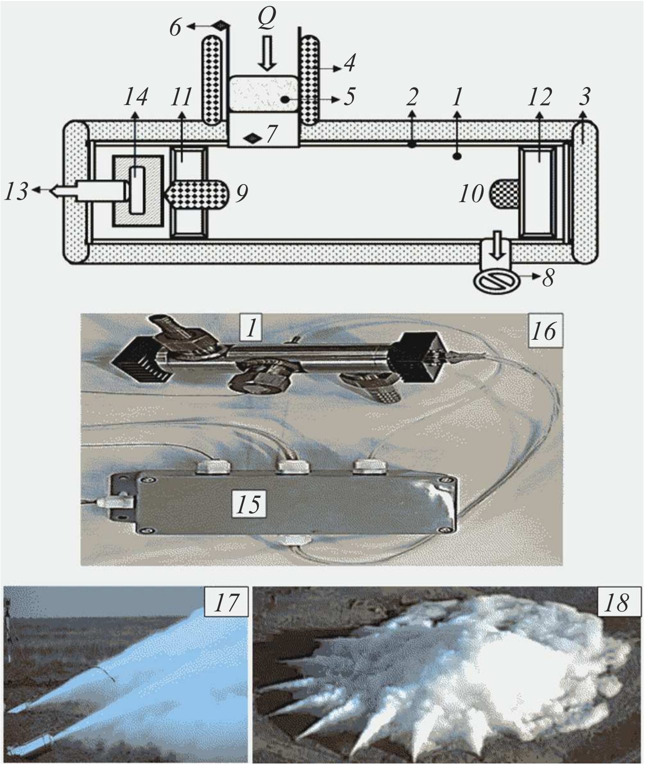

Figure 1. Principle diagram and image of the low-temperature IR gas analyzer based on the immersion diode optocouplers: *1* — the measurement gas cuvette with the body *2* and the external *3* heat-insulation coating; *4* — the cylindrical electric oven with the aerosol metal filer *5* therein; *6* and *7* — the thermocouples for measurement of the temperature of the gas-carbon mixtures outside and inside the IR gas analyzer; *8* — the flow activator Q of the analyzed air-carbon mixture; *9* and *10* — the immersion light-emitting diode and photodiode, respectively; *11* and *12* — the adjusting elements thereof; *13* — the connector for connection of the external electronic unit *15* designed to connect the circuits of control, power supply and data transmission; *14* — the system of thermal stabilization of the immersion light-emitting diode and photodiode; *16* — the image of the external electronic unit *15* and the gas cuvette *1* without the heat-insulation coating *3*; *17* and *18* — the images of emission of flooded LNG jets from nozzles at the initial velocity and the length 60 m/s and 50 m, with formation of the cold carbon-air cloud of the volume about 10^5 m^3, spreading above the ground surface.

The light-emitting diode *9* and the photodiode *10* are tuned by the adjusting elements *11* and *12* to the maximum output signal of the photodiode *10*. Both the semiconductor devices with the operating wavelength of $\lambda \approx 3.2-3.6\,\mu$m are provided with the thermal stabilization system *14* based on the Peltier elements to keep its temperature at the given level from 285 to 300 K. The values T are read by an analogue-digital converter (ADC) of the microprocessor for control and together with the light and background signals of the photodiode *10* they are sent by the RS-485 interface to the remote server (not shown on Fig. 1). The optical length L and the volume of the gas cuvette *1* are about 0.1 m and $2.8 \cdot 10^{-6}\,\mathrm{m}^3$.

In accordance with the Beer-Lambert-Bouguer law, the attenuation of the intensity of radiation passed through the multi-component AFM is

$$I = I_0 \exp\left(-L \sum \Delta_i C_i\right),$$

where I_0 and I — the monochromatic radiation intensities before and after AFM, respectively, L — its optical length, Δ_i — the spectral absorption coefficient for radiation of the i-component AFM, C_i — its concentration. Its absorbance can be calculated based on the additive law as

$$D = \lg(I_0/I) = \sum D_i,$$

where $D_i = \lg(I_0/I_i)$ — the absorbance of the AFM i-component with attenuation of radiation I_i [16,17].

It is known that the LNG temperature at the normal storage conditions is about 110 K, and the composition of its LHWF flammable components is not rated, but their main volume content is determined by the concentration of ethane, propane and butane [18]. When the liquified gas is emitted into the atmosphere, there is a reduced temperature of the carbohydrate cloud. For example, in large-scale jet LNG emission of the weight up to $5 \cdot 10^3 - 10^4$ kg, there was evident temperature reduction to 160 K in the center of the AFM cloud of the volume above $10^5\,\mathrm{m}^3$ [10,11]. In this regard, before being supplied into the gas cuvette *1*, the flux of the analyzed AFM is preheated in the electric oven *4* with the aerosol copper filter *5*. Its optimum flowrate $Q \approx (3-9) \cdot 10^{-4}\,\mathrm{m}^3/\mathrm{s}$.

The characteristics of the IR gas analyzer with the light-emitting diode *9* of the LED34TO8TEC grade and the photodiode *10* of the PD34TO8TEC grade with $\lambda = 3.4\,\mu\mathrm{m}$ [12-14] were calibrated and analyzed on a gas test bench by creating the given volume concentration of alkanes or LNG with filtered air with their homogeneous mixing in screw-corrugation pipes [10,11,15]. The carbohydrate concentration was determined from the relationship of the volume flowrates of alkanes or LNG and air with periodic chromatographic analysis of their samples. In doing so, it also included using methane, ethane, propane and butane with $C > 99.95$ vol.%, as well as industrial domestic LNG with the LHWF concentration from 2 to 7 vol.% [18].

The large-scale LNG emissions of the weight up to $5 \cdot 10^3$ kg were analyzed when it was sprayed as the flooded jets being split at the numbers of Reynolds $\mathrm{Re} = Vd\rho/\eta < 10^5$ and Weber $\mathrm{We} = \rho(V - V_0)^2 d/\sigma < 10^4$ with vaporization of boiling drops [1,2,17]. The convective heat exchange between them and the atmosphere was determined by the state of air medium, the temperature and the wind speed, as well as the size of the AFM cloud. Here, ρ, η and V_0 — the density, the dynamic viscosity, air speed, respectively, $\sigma = 15.5 \cdot 10^{-3}$ n/m — the LNG surface tension coefficient at 110 K, $d \leq 0.05$ m — the LNG drop diameter, $V \leq 60$ m/s — their velocity. In doing so, the jets and the AFM cloud are evidently visualized (the image *17*, Fig. 1) due to spontaneous condensation of water vapors being sharply cooled with formation of the water fog of drops and ice particles. The initial relative humidity of air was 35–40% at $T \approx 280-285$ K.

2. Results and discussion thereof

Figure 2 shows the dependence of the voltage U at the photodiode signal amplifier output *10* on the time t when switching on and off the light-emitting diode *9* (LED34TO8TEC) with the duration of its switched-on state of $130\,\mu$s in order to determine the speed τ_0 of the electronic unit of the IR gas analyzer. During its measurement, the microprocessor timer was set for the repetition period of 20 ms. By interruption of the timer at $t = -80\,\mu$s, with the switched-off light-emitting diode, its ADC reads the photodiode background signal 16 times to obtain an averaged value. At the time $t = 0\,\mu$s, the microprocessor switches on the light-emitting diode and in $52\,\mu$s after full stabilization of its IR radiation, the microprocessor ADC reads the photodiode signal level 16 times, too, to obtain the averaged light value. Then, the microprocessor switches off the light diode and the measured values U are transmitted to the server at the distance of 1200 m. The analysis of the data of Fig. 2 has shown that $\tau_0 \leq 25\,\mu$s.

Figure 3 shows the dependence of the relative change of the voltage U_t/U_1 at the photodiode signal amplifier output *10* (PD34TO8TEC) on the time t in exchange in more than 100 times per second in the methane gas analyzer with the initial concentration of $C = 6.5$ vol.% by the filtered air with the flowrate $Q = 9 \cdot 10^{-4}\,\mathrm{m}^3/\mathrm{s}$, in order to determine its speed, where U_1 — the stationary voltage at the photodiode signal amplifier output at $C = 6.5$ vol.%, U_t — the change of the voltage at the photodiode signal amplifier output on time during methane exchange with air in the gas cuvette and, respectively, the decrease in its concentration from 6.5 to ≈ 0.6 vol.%. The analysis of the

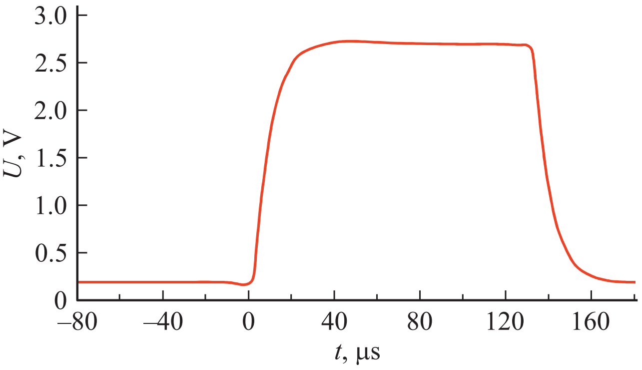

Figure 2. Dependence of the voltage U of the photodiode signal amplifier on the time t.

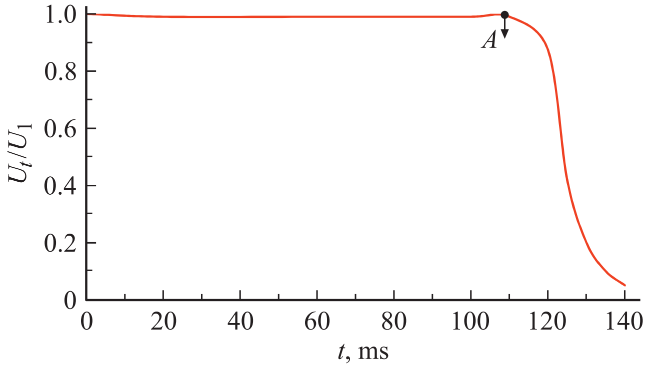

Figure 3. Dependence of the relative change of the voltage U_t/U_1 at the output of the photodiode signal amplifier on the time t; A — the start of exchange at $t \approx 110$ ms.

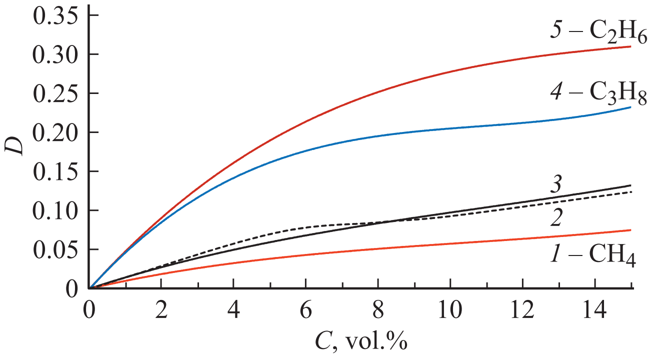

Figure 4. Experimental dependence of the values of the absorbance D of the mixture of air with the alkanes and LNG on the value of its volume concentration C: *1* — methane, *2* — the calculation of D for LNG as per the additive law, *3* — LNG, *4* — propane, *5* — ethane.

data of Fig. 3 has shown that the value $\tau \leq 25-30$ ms at $\tau_0 \approx 25\,\mu$s.

The dependences of the values D measured for the mixture of air with methane, regasified LNG, propane and ethane (the solid curves *1, 3–5*, respectively) on their volume concentration C are shown on Fig. 4. Note that at $C < 1$ vol.% the values D are the same with accuracy, which is sufficient for practical purposes. The dashed curve *2* — the calculated values D for LNG as a sum of the measured values of the absorbances of the D_i alkanes included it its composition with a known volume concentration: 93 methane, 4.8 ethane, 1.5 propane, 0.5 butane and 0.2 vol.% other impurities [18]. It should be noted that the curves *2* and *3* satisfactorily coincide.

The analysis of vaporization of the emissions of the alkanes and LNG into the atmosphere also included the calculations of the time t of full evaporation and 50% evaporation of the weight of the cryogenic drops on their diameter $d = 10-5000t\,\mu$ at the air temperature of $T = 112-293$ K. The values t have been calculated based on the experimentally proved model of convective energy exchange between the cryogenic drop and the surrounding vapor-gas medium during its fall in air at the temperature from 112 to 293 K at the Reynolds numbers $\mathrm{Re} = d\rho V_S/\eta \approx 0.1-10^5$, where V_S — the drop sedimentation rate [10,19,20]. The drop evaporation process is non-stationary and proceeds in a liquid boiling mode with the constant temperature to its vaporization. The non-stationary convective mass transfer in the gas phase in evaporation is correlated to loss of stability of the diffusion mode at the initial phase of drop motion. The drop sedimentation rate has been determined by the known dependences at $\mathrm{Re} < 1$ (the Stokes law) in the transient mode ($1 < \mathrm{Re} < 10^3$) and in the applicability region of the Newton's law ($10^3 < \mathrm{Re} < 10^5$) [17–20]. As a result, for the boiling drop, we have obtained the dependence of the change of d on t taking into account the liquid evaporation heat at $\mathrm{Re} < 10^5$. In doing so, neither drop deformation, nor radiative heat exchange was taken into account. Note that using the classical diffusion evaporation theory of Maxwell-Langmuir as well as Knudsen and Hertz for the boiling drops immobile in relation to the vapor-gas medium [17–20] is not correct, as their temperatures are substantially different, and the drops themselves sediment.

As an example, Fig. 5 shows the values of the time t of the full evaporation of the cryogenic drops of alkanes of the diameter $d = 10-500\,\mu$m at $T = 293$ K. It follows from the data of Fig. 5 that the methane drops evaporate faster than the drops of the heavier alkanes. The similar result was at reduction of the temperature to 150 K as well as during evaporation of two-component cryogenic drops of methane with an impurity of ethane or propane with the concentration from 1 to 10 vol.%. The obtained results agree with the experimental data about the predominant vaporization of methane (boil-off gas) in large-sized vessels for storage and transport of LNG [21], as well as with observation of no formation of substantially heterogeneous mixtures of ethane, propane and butane in the carbon-air clouds when LNG is emitted as jets or ground spills with its subsequent regasification [10,11].

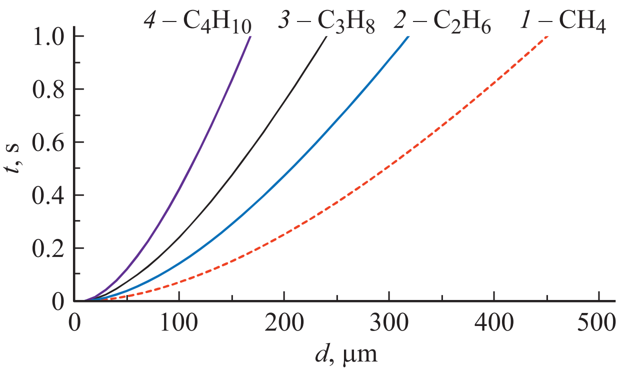

Figure 5. Dependence of the calculated values of the time t for full evaporation of the cryogenic drops of alkanes at the air temperature of 293 K on their diameter d: *1* — methane, *2* — ethane, *3* — propane, *4* — butane.

Note that the value $t < 1$ s for the methane drops of the diameter below $500\,\mu$m. The time of reduction of its diameter by 20% with evaporation of the 50% mass is substantially less, and, for example, for the methane drops of the diameter of $d = 100$, 500 and $1000\,\mu$m it is ≈ 0.04, 0.56 and 1.6 s, respectively, at $T = 293$ K. Many IR analogues with the time resolution above 0.3 s [4–10] are not designed to detect the process of so fast vaporization of fine cryogenic drops of the alkanes and LNG (Fig. 5). The manufactured IR gas analyzer based on the immersion diode optocouplers was capable of analyzing their vaporization with the speed $\tau < 0.03$ s. It is required, in particular, for engineering analysis of the large-scale pulse LNG outflows due to using the high-energy materials with formation of the explosive and fire hazardous AFMs of the volume above $10^5\,m^3$ for several seconds.

It has been demonstrated that in large-scale LNG emissions the carbon-air cloud exhibits therein local and explosive AFMs of the volume from 10^3 to $10^5\,m^3$ with the volume concentration of the carbohydrate vapors from 5 to 15 vol.%. The duration of their existence depends on the spraying conditions and a mass of the pulse emitted LNG as well as on the condition of the atmosphere and a soil. During evaporation of the sprayed LNG and increase in the concentration of its vapors, the AFM temperature in the cloud center was reduced to 150−170 K. At the same time, inside the IR gas analyzer, the temperature was almost the same to be about 290 K. The concentration and the temperature of the gas mixtures of methane, LHWF and air vapors fluctuated in time and were heterogeneously distributed both along the height (up to 40 m) and along the length (more than 100 m) of the clouds. We have obtained the data on the kinetics of the change of the temperature from 280 to 150 K and the methane concentration from 1 to 30 vol.%. inside the LNG clouds of the volume of up to $10^6\,m^3$ with transmission of the data with an interval of 1 ms to the master server at the distance of 4000 m. These data qualitatively correlate to the data of the „Falcon" experiments for LNG outflow into the atmosphere [2,3].

Conclusion

The IR gas analyzer has been developed and patented based on the immersion diode optocouplers with the speed below 0.03 s at $T > 150$ K. It is designed to determine the volume concentration of alkanes and LNG vapor during their man-made emission into the atmosphere as jets and ground spills with transmission of the digitalized data along the fiber-optic line to the remote server. Its technical characteristics exceed the parameters of domestic and foreign gas analyzer for analysis of emergency LNG emissions.

The manufactured high-speed IR gas analyzer can be used for express control of alkane and LNG CILs in their pulse emission into the atmosphere by means of high-energy materials for fast AFM development, as well as in technologies of creating gas drop fluxes of alkanes in the large-scale methane-air mixtures of LNG when studying their explosive and fire hazardous properties.

A network of the IR gas analyzers can be integrated into the industrial safety express systems of the fuel and energy sector for obtaining and storage of LNG, as well as for analysis of evolution of their emissions with formation of the large-scale AFM clouds.

Funding

The study has been performed on the subject „Development of physical and technical methods of measurement of parameters of aerosol and vapor-gas clouds occurring in large-scale emergencies on fuel and energy facilities and creation of experimental samples of the systems of diagnostics of aerosol clouds" as per the order № 2748 dated October 28, 2021.

Conflict of interest

The authors declare that they have no conflict of interest.

References

[1] C.J.R. Coronado, J.A. Carvalho, J.C. Andrade, E.V. Cortez, F.S. Carvalho, J.C. Santos, A.Z. Mendiburu. J. Hazardous Mater., **2414**−**4242**, 32 (2012). doi:org/10.1016/jhazmat.2012.09.035
[2] S.T. Chan. J. Hazardous Mater., **30**, 195 (1992).
[3] T.C. Brown, R.T. Cederwall, S.T. Chan, D.L. Ermak, R.P. Koopman, K.C. Lamson, D.L. Ermak, R.P. Koopman, K.C. Lamson, J.W. McClure, L.K. Morris. Lawrence Livermore National Lab., 665 (1990).
[4] V.V. Malyshev, A.V. Pislyakov. Zhurn. analit. khimii, **64** (1), 99 (2009) (in Russian).
[5] Z.Maolin, Y. Zhanheng, S. Jianping, Z. Cheng. J. Sensors Actuators B, **148**, 87 (2010).
[6] A.A. Vasiliev, V.V. Malyshev. J. Sensors Actuators B, **189**, 260 (2013).
[7] *Sistema gazoanaliticheskaya SKVA-01, EKRM.411741.001RE, Rukovodstvo po ekspluatatsii* (OOO NPF INKRAM, M., 2013), 58 p. (in Russian).
[8] *Gazoanalizatory serii Sensis* (OOO Delta-S, M., 2008) (in Russian).
[9] *Malogabaritnyi izmeritel'nyi preobrazovatel' vzryvoopasnykh gazov MIP. Rukovodstvo po ekspluatatsii* (OOO Optosens, SPb, 2012), 50 p. (in Russian).
[10] A.V. Zagnit'ko, N.P. Zaretskiy, I.D. Matsukov, V.I. Alekseev, S.M. Vel'makin, D.Yu. Fedin, V.V. Pimenov, S.E. Sal'nikov. Zhurn. gazovaya promyshlennost', (5), 82 (2021) (in Russian).
[11] A.V. Zagnit'ko, N.P. Zaretskiy, I.D. Matsukov. ZhFKh, **94** (9), 1328 (2020) (in Russian).
[12] OOO „IoffeLed". www.ioffeled.com
[13] S.E. Aleksandrov, G.A. Gavrilov, A.A. Kapralov, B.A. Matveev, G.Yu. Sotnikova, M.A. Remennyi. Tech. Phys., **54** (6), 874 (2009).

[14] S.A. Karandyshev, B.A. Matveev, M.A. Remennyi, A.A. Shlenskiy, L.S. Lunin, V.I. Ratushnyi, A.V. Koryuk, N.G. Tarakanova. FTP, **41** (11), 1389 (2007) (in Russian).

[15] A.V. Zagnit'ko, D.Yu. Fedin. *Nizkotemperaturnyi infrakrasnyi analizator vybrosov parov szhizhennogo prirodnogo gaza v atmosphere na osnove immersionnykh diodnykh optopar* (Patent RF na poleznuyu model. № 201917. Bulletin 3, dated January 21, 2021) (in Russian).

[16] G.S. Landsberg. Optika (Nauka, M., 1976), 928 p. (in Russian).

[17] P. Raist. *Aerosoli, vvedenie v teoriyu* (Mir, M., 1987), 280 p. (in Russian).

[18] GOST R 57431-2017. Liquefied natural gas. General characteristics. https://docs.cntd.ru/document/1200144948

[19] Y. Ruan, L. Chen, X. Liu, S. Chen. IOP Conf. Ser.: Mater. Sci. Eng., **278**, 8 (2017). DOI: 10.1088/1757-899X/278/1/012130

[20] S.O. Awonorin. J. Heat Transfer Eng., **10** (1), 26 (1989). DOI: 10.1080/01457638908939689

[21] E.S. Seredenko, O.V. Pakhomov, A.Yu. Baranov. Scientific and Technical Bulletin of Information Technology, Mechanics and Optics, **20** (4), 603 (2020). DOI: 10.175862226-1494-2020-4-603-610